

# SDOD: Real-time Segmenting and Detecting 3D Objects by Depth

Caiyi Xu<sup>1</sup>, Jianping Xing<sup>1\*</sup>, Yafei Ning<sup>1</sup>, YongHong Chen<sup>2</sup>, Yong Wu<sup>2</sup>

<sup>1</sup>School of Microelectronics, Shandong University, Jinan, China

<sup>2</sup>City Public Passenger Transport Management Service Center of Jinan, Jinan, China

cyxu@mail.sdu.edu.cn, {xingjp, ningyafei}@sdu.edu.cn, chenyhjn@foxmail.com, wu.100@163.com

## Abstract

Most existing instance segmentation methods only focus on 2D objects and are not suitable for 3D scenes such as autonomous driving. In this paper, we propose a model that splits instance segmentation and object detection into two parallel branches. We discretize the objects depth into “depth categories” (background set to 0, objects set to  $[1, K]$ ), then the instance segmentation task has been transformed into a pixel-level classification task. Mask branch predicts pixel-level “depth categories”, 3D branch predicts instance-level “depth categories”, we produce instance mask by assigning pixels which have same “depth categories” to each instance. In addition, in order to solve the problem of imbalance between mask labels and 3D labels in the KITTI dataset (200 for mask, 7481 for 3D), we use unreal mask generated by other instance segmentation method to train mask branch. Despite the use of unreal mask labels, experiments result on KITTI dataset still achieves state-of-the-art performance in vehicle instance segmentation.

## 1 Introduction

Instance segmentation and 3D object detection from a RGB image are key tasks for autonomous driving, they help autonomous vehicles perceive complex surroundings. Instance segmentation is a combination of object detection and semantic segmentation, so it can be perfectly integrated with 2D object detection tasks, and this is what Mask RCNN[He *et al.*, 2017] has done. What about merging instance segmentation with 3D object detection tasks?

Different from 3D instance segmentation based on point cloud, our goal is to propose a network that when we input a image it can outputs 3D location, 3D bounding box and instance mask, as shown in Fig. 1.

State-of-the-art approaches to instance segmentation like Mask RCNN [He *et al.*, 2017] and FCIS[Li *et al.*, 2017] are two-stages, they focus on performance over speed. We focus on speed over performance, and propose a network that can segment instance and detect 3D objects by depth in real-time.

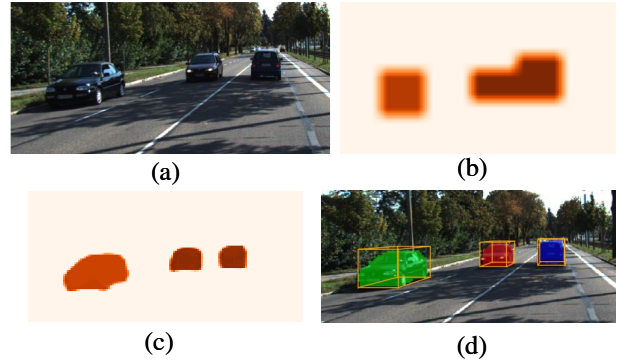


Figure 1: **Input and output** Fig.(a) input of SDOD; Fig.(b) instance-level depth categories map; Fig.(c) pixel-level depth categories map; Fig.(d) fused instance segmentation and detection output. In Fig (b) and (c) darker the color of a pixel/instance is, the greater the depth value of a pixel is, and the farther the pixel/instance is from us.

It is known to all that 2D detection is faster than 3D detection, semantic segmentation is faster than instance segmentation. Some state-of-the-art 3D objects detection frameworks speed up by splitting 3D tasks into multiple 2D related sub-tasks. [Qin *et al.*, 2019] propose a network composed of four task-specific subnetworks, responsible for 2D object detection, instance depth estimation, 3D localization and local corner regression. Inspired by this idea, we split 3D detection task into these four sub-tasks.

Now, there are three challenges left: 1) how to transform instance segmentation tasks into semantic segmentation tasks 2) how to combine 3D network with instance network efficiently 3) how to train 3D networks and instance network together.

We use depth to connect the 3D network with the instance network, and at the same time we use depth to transform instance segmentation into semantic segmentation. We believe that different instances have different depths. If they have the same depth, they are spatially separated. For example, if two cars in the image are obscured or overlapped, they mask have different depth, if they have same depth, we can distinguish them by 2D bounding box.

As shown in Fig. 2, we divide the network into two parallel branches: 3D branch and mask branch. We discretize

\*Contact Author

the objects depth into “depth categories”, 3D branch predicts instance-level depth categories, mask branch predicts pixel-level depth categories. In this way, mask branch classifies each pixel, this is similar to semantic segmentation. Finally, we produce instance mask by assigning pixels which have same “depth categories” to each instance.

The instance segmentation labels in the KITTI dataset are not balanced with the 3D detection labels(200:7841), so we cannot train 3D and mask branches directly. First We use the instance segmentation model trained on Cityscapes provided by [Acuna *et al.*, 2018] to generate unreal masks on the KITTI dataset. Then add real depth to these unreal masks. Finally we use these masks to train mask branch.

Different from two-stage instance segmentation method, the 3D branch and mask branch of our network are parallel and proposal-free. This is the main reason that our network is real-time. Experiments on the KITTI dataset demonstrate that our network is effectively and real-time.

In general, our contributions of this paper are three-fold:

- Transform instance segmentation tasks into semantic segmentation tasks by discretizing depth.
- Propose a network that combines 3D detection and instance segmentation and set them as parallel branches to speed up.
- Combine unreal masks with real depth to train mask branch to solve the problem of imbalanced labels.

The remainder of this paper is organized as follows: related works are introduced in Sec.2. Our method is well illustrated in Sec. 3. In Sec. 4, we conduct experiments to verify the effectiveness of the proposed framework. Finally, we conclude this paper in Sec.5.

## 2 Related Work

Our work is related to 3D object detection, depth estimation and instance segmentation. We mainly focus on the works of studying 3D detection, depth estimation and instance segmentation, while 2D detection is the base for them.

**2D Object Detection** 2D object detection methods based on convolutional neural networks[Krizhevsky *et al.*, 2012] are mainly divided into one stages and two stages. Two stages method [Ren *et al.*, 2015] use region proposal to generate ROI, performance well but slowly. One stage method [Redmon *et al.*, 2016] and [Liu *et al.*, 2016] focus on speed over performance, they are faster but less accurate. Methods above are anchor based, [Tian *et al.*, 2019] use no anchor and performance better than anchor based methods. Multinet [Teichmann *et al.*, 2018] proposes a non-proposed approach similar to YOLO, and uses RoiAlign[He *et al.*, 2017] in rescaling layer to narrow the gap, we use this as our 2D detector.

**3D Object Detection** Existing methods based on RGB image includes multi-view methodcitechen2017multi, single-view method[Qin *et al.*, 2019], [Bao *et al.*, 2019] and RGB-Depth method. multi-view RGB method[Chen *et al.*, 2017] takes the bird’s eye view and front view of point cloud as well as an image as input, RGB-Depth method takes RGB image and

point cloud depth as input, single-view method MonoGRNet takes a single RGB image as input. MonoGRNet proposes a network composed of four task-specific subnetworks, responsible for 2D object detection, instance depth estimation, 3D localization and local corner regression. We need a simple and real-time 3D detection method, and the input must be a single RGB image. Inspired by MonoGRNet, we split 3D detection task into these four sub-tasks.

**Depth Estimation** Depth estimation is mainly divided into monocular depth estimation and binocular depth estimation. Binocular depth estimation[Kendall *et al.*, 2017] uses the disparity of two image to estimate depth. Monocular depth estimation directly estimates the depth of each pixel. [Fu *et al.*, 2018] proposes a spacing-increasing discretization method to discretize continuous depth values, and transform depth estimation task into classification task. This method estimates the depth of each pixel in the image, it may not suitable for 3D object detection. In the 3D branch, we estimate instance-level depth, which is the center depth of the object, and in the mask branch, we estimate pixel-level depth.

**Instance Segmentation** Existing methods range from one-stage instance segmentation approach YOLACT[Bolya *et al.*, 2019]; SOLO[Wang *et al.*, 2019] to two-stage instance segmentation approach Mask-RCNN[He *et al.*, 2017], Mask scoring r-cnn[Huang *et al.*, 2019]. Mask-RCNN is a representative two-stage instance segmentation approach that first generates ROI(region-of-interests) and then classifies and segments those ROI in the second stage. Mask scoring r-cnn is an improvement on Mask R-CNN. Add a new branch to Mask R-CNN to score the mask to predict a more accurate score.

Similar to two-stage object detection, two-stage instances are based on proposal, they performance well but slowly. SOLO distinguish different instances by 2D location. SOLO divided an input image of  $H \times W$  into  $S_x \times S_y$  grids, and do semantic segmentation in each grid, this is similar to the main idea of YOLO. However, it only uses 2D location to distinguish different instance, performance not good for overlapped instance.

We discretize the object depth into “depth categories” (background set to 0, objects set to [1, K]), 3D branch predicts instance-level depth categories, mask branch predicts pixel-level depth categories. In this way, mask branch classifies each pixel, this is similar to semantic segmentation. Finally, we produce instance mask by assigning pixels which have same “depth categories” to each instance.

## 3 SDOD

In this section, we first introduce the overall structure of the proposed SDOD framework, as shown in Fig. 2, which consists of two parallel branches, a 3D branch and a mask branch, and then detail these two branches.

### 3.1 3D Branch

We leverage the design of MonoGRNet[Qin *et al.*, 2019], which decomposes the 3D objects detection into four sub-

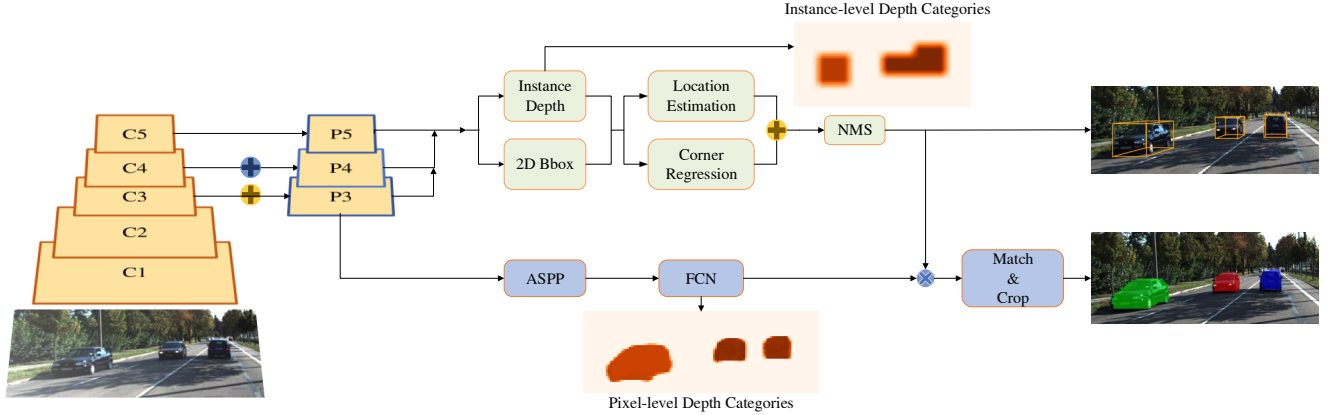


Figure 2: **SDOD Architecture** SDOD consists of a backbone network (brown) and two parallel branches: a 3D branch (green) and a mask branch (blue). SDOD takes an image and outputs 3D object detection and instance segmentation results.

networks: 2D detection, instance-level depth estimation, 3D location estimation and corners regression.

### 2D Detection

The 2D detection module is the basic module that extracts the region of interest from the feature map, classifies the object and regresses bounding boxes.

We use the design of detection in [Teichmann *et al.*, 2018], which proposes a non-proposed approach similar to YOLO [Redmon *et al.*, 2016] and Overfeat [Sermanet *et al.*, 2013]. To archive the good detection performance of proposal based detection systems, it uses RoiAlign [He *et al.*, 2017] in rescaling layer. An input image of  $H \times W$  is divided into  $S_x \times S_y$  grids, and each grid is responsible for detecting objects whose center falls into the grid. Then each grid outputs the 2D bounding box  $B_{2d}$  and the class probabilities  $P_{cls}$ .

### Instance-Level Depth Estimation

Given a grid  $g$ , this module predicts the center depth  $g_d$  of the object in  $g$  and provides it for 3D location estimation and mask branch.

It is hard to directly regress the center depth  $g_d$ , we discretize the continuous depth, and a particular class  $c$  can be assigned to each depth  $d$ . We use the following formula provided by [Fu *et al.*, 2018] to convert the depth  $d \in [\alpha, \beta]$  to category  $c_i$ ,  $i \in [0, K - 1]$ :

$$c_i = e^{\log(\alpha) + \frac{\log(\beta/\alpha) * i}{K}} \quad (1)$$

As shown in Fig. 2, the module takes P5 and P4 as the input feature map. Compared with P4, P5 has larger receptive field and lower resolution, it is less sensitive to location so we use P5 to generate a coarse depth estimation, and then fused with P4 to get accurate depth estimation.

Compared with the pixel-level depth estimation of the mask branch, the resolution of the module output is lower, which is an instance-level. For details of implementation, please refer to section 3.2.

### 3D Location Estimation

The 3D location module uses the 2D coordinates  $(u, v)$  and the center depth  $d$  of the object to calculate the 3D location  $(x, y, z)$  by the following formula:

$$\begin{cases} u = x \cdot f_x + cx \\ v = y \cdot f_y + cy \\ d = z \end{cases} \quad (2)$$

$f_x, f_y, cx, cy$  are camera parameters which can be obtained from the camera's internal parameter matrix  $C$ .

### Corners Regression

We first establish a coordinate system whose origin is the object center, and the  $x, y, z$  axis is parallel to the camera coordinate axis, and then regress the 8 corners of the object. Finally, we use the method of [Mousavian *et al.*, 2017] to calculate the object's length, width, height, and observation angle from 8 corner points.

### 3.2 Mask Branch

The Mask branch predicts pixel-level depth categories over the entire image, which is similar to semantic segmentation. Semantic segmentation is classified according to the target category to which the pixel belongs, and Mask branch are classified according to the depth category to which the pixel belongs. As shown in Fig. 2, the Mask branch consists of an ASPP module and an FCN module, and these two modules are also common modules for semantic segmentation tasks.

#### ASPP

The input of the ASPP module is the P3 feature map, and its resolution is only 1/8 of the original image. In order to expand the receptive field of the input and obtain more semantic information, we use the ASPP module, inspired by [Yu and Koltun, 2015].

As shown in Fig. 3, The ASPP module connects 1 convolutional layer and 3 dilated convolutional layers, and outputs it to the FCN module after a convolutional layer. The input size of the module is  $156 \times 48 \times 256$ , the output size after concatenated

is  $156 \times 48 \times 512$ , and the output size after  $1 \times 1$  convolutional is  $156 \times 48 \times 256$ .

### FCN

To get a pixel-level depth category map, we use a FCN module which is similar to mask branch in [He *et al.*, 2017], proposed by [Long *et al.*, 2015]. As shown in Fig 4, compared to [He *et al.*, 2017] we have added a  $1 \times 1$  convolution layer, which is responsible for depth classification of each pixel.  $K$  is the total number of depth categories in Equation 1, we set it to 64, and  $C$  is the number of target categories, we set it to 3(car person cyclist).

The FCN module finally outputs  $C$  images, each image is a pixel-level depth category map of the target, as shown in Fig. 2. The darker the color of a pixel is, the greater the depth value of a pixel is, and the farther the pixel is from us. The size of the output image is  $312 \times 96$ , and the size of the original image is  $1248 \times 384$ .

### 3.3 Match And Crop

Instance segmentation requires each pixel to be assigned to a different instance. We need to assign each pixel in the pixel-level depth map  $X = \{x_0, x_1, x_2 \dots x_{N-1}\}$  to a set of instance  $C = \{c_0, c_1, c_2 \dots c_{M-1}\}$  in the 3D branch.

This is a pixel clustering task. Unlike the pixel clustering method used by [Neven *et al.*, 2019], we use the depth of the pixel as a constraint for clustering:

$$x_i \in c_k \Leftrightarrow |x_i - c_k| < \delta_k \quad (3)$$

$x_i$  is the pixel depth category,  $c_k$  is the depth category of the instance, and  $\delta_k$  is the clustering threshold of the instance.

We must be clear that each instance has only one depth category in the instance-level depth map, but each instance may have multiple depth categories in the pixel-level depth map. So we set a depth threshold for each instance  $\delta_k$ , which is calculated by the following formula:

$$\begin{aligned} \delta_k &= \text{map}(L_k \cdot \cos \theta_k, z_k), \\ \text{map}(a, b) &= K \times \log_{\beta/\alpha}(1 + a/b) \end{aligned} \quad (4)$$

$L_k$   $z_k$  and  $\theta_k$  are the length depth and observation angle of the target, which can be obtained from the corners regression module. Crop operation means using the 2D bounding box to crop the final instance mask, and this can improve the accuracy of the mask. During training, we use truth bounding boxes to crop the predicted mask.

### 3.4 Loss Function

Here we have determined independent loss functions for each module and joint loss functions for the entire network.

**2D Detection Loss.** 2D detection includes classification loss  $L_{cls}$  and box regression loss  $L_{box}$ , they are defined in the same as in [Teichmann *et al.*, 2018]. Due to the imbalance of samples between classes in the KITTI dataset, we used focal loss [Lin *et al.*, 2017b] to modify the classification loss. The total loss of 2D inspection is

$$L_{2d} = w_1 L_{cls} + w_2 L_{box} \quad (5)$$

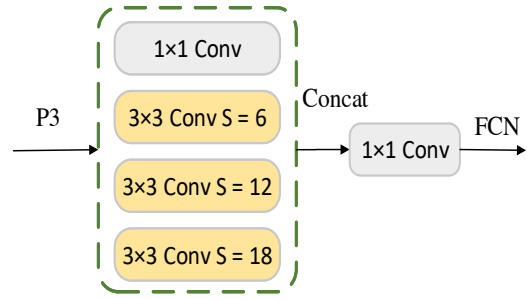


Figure 3: **ASPP Architecture** The ASPP module consists of 1 conv layers with with kernel size of  $1 \times 1$  (gray) and 3 dilated conv layers with kernel size of  $3 \times 3$  (brown) and dilated rate of 6, 12 and 18 respectively.

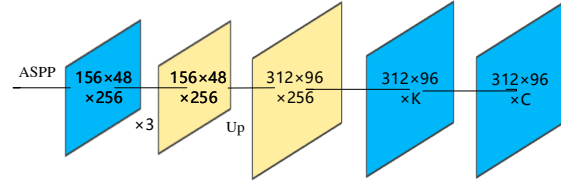


Figure 4: **FCN Architecture** The brown feature map is obtained by  $3 \times 3$  conv, and the blue feature map is obtained by  $1 \times 1$  conv.  $\times 3$  means that 3 conv layers are used, Up means that upsampling layer is used.

where  $w_1$  and  $w_2$  are weight coefficients, when we trained 2D detection only, we set  $w_1 = w_2 = 1$ .

**Instance-Level Depth Loss.** We use L1 loss as instance-level depth loss:

$$L_d = \sum_{i=1}^n |d_i - \hat{d}_i| \quad (6)$$

where  $n$  is the number of cell,  $d_i$  is the ground truth of cell  $i$ ,  $\hat{d}_i$  is the prediction of cell  $i$ .

**Corner Loss And Location Loss.** We use L1 loss as corner loss and location loss, and they are the same as in [Qin *et al.*, 2019].

**Pixel-Level Depth Loss.** Different from the cross-entropy (CE) loss function used in semantic segmentation tasks, we use the L1 loss the same as the instance-level depth loss.

$$L_{mask} = \sum_{i=1}^m |M_i - \hat{p}_i| \quad (7)$$

where  $n$  is the number of pixel,  $M_i$  is the ground truth of pixel-level depth categories, which is defined by Equation 8,  $p_i$  is the prediction category of pixel  $i$ .

We also tried L2 loss, CE loss and Focal loss, and finally we found that L1 loss performed better. We think that the smaller the object is, the farther it is, the greater its depth value is and the greater the loss is. And this is why long-distance object can be detected well.

## 4 Experiments

Note that only the KITTI dataset [Geiger *et al.*, 2012] has both 3D object detection and instance segmentation challenging in the main autonomous driving dataset, Cityscapes and BDDV datasets are lack of 3D data. So we evaluate our network on the KITTI dataset.

### 4.1 Datasets and Settings

#### Datasets

The KITTI dataset has 7841 training images and 7581 test images with calibrated camera parameters for 3D object detection challenge. However, due to the difficulty of instance segmentation labeling, there are only 200 labeled training images and 200 unlabeled testing images for instance segmentation challenge. In addition, the 3D object detection task evaluates on 3 types of targets(car, person, cyclist), and instance segmentation task evaluates on 8 types of targets(car, person, cyclist, truck, bus, train, bicycle, motorcycle).

We think that car is the main vehicle in the autonomous driving scenes, motorcycle, bicycle and cyclist can be merged into 1 category, so only car, cyclist, and person will be detected by our network. We evaluate cars, people, and cyclists on both 3D object detection and instance segmentation tasks

#### Settings

in order to solve the problem of imbalanced between mask labels and 3D labels in the KITTI dataset, we use unreal mask generated by other instance segmentation method to increase samples of instance segmentation. We use the instance segmentation model trained on Cityscapes provided by [Acuna *et al.*, 2018] to generate unreal masks on the KITTI dataset. We use 200 labeled training images to evaluate the accuracy of the unreal mask, results are shown in Table 1. We did not directly train the Mask branch with unreal labels, but superimposed the real depth value with it for training:

$$M_i = c_i \times M_{ei} \quad (8)$$

$c_i$  is the depth category of instance  $i$ , which can be calculated from Equation 1.  $M_{ei}$  is the unreal mask of instance  $i$ , with a value of 0 or 1,  $M_i$  is the training label for mask branch.

|      | car   | person | cyclist | average |
|------|-------|--------|---------|---------|
| AP   | 0.401 | 0.363  | 0.351   | 0.372   |
| AP50 | 0.567 | 0.506  | 0.503   | 0.525   |

Table 1: Unreal Mask Accuracy

#### Evaluation Metrics

For evaluating 3D detection performance, we follow the official settings of KITTI benchmark to evaluate the 3D Average Precision ( $AP_{3d}$ ). For evaluating instance segmentation performance, we follow the official settings of KITTI benchmark to evaluate the Average Precision on the region level ( $AP$ ) and Average Precision with 50% ( $AP50$ ). Note that we only evaluate three types of object: car, person, and cyclist, the reason has been discussed in the Dataset section.

### 4.2 Implement Details

**Network.** The architecture of SDOD is shown in Figure 2. VGG-16 [Simonyan and Zisserman, 2014] and FPN [Lin *et al.*, 2017a] are employed as the backbone.

**Training.** 2D detector should be trained first, we set  $w_1 = w_2 = 1$  in the loss functions and initialize VGG-16 with the pretrained weights on ImageNet. We trained 2D detector for 150K iterations with the Adam optimizer [Kingma and Ba, 2014], and L2 regularization is used with a decay rate  $1e-5$ . Then 3D branch and mask branch are trained for 120K iterations with the Adam optimizer. We set batch size to 4 and learning rate to  $1e-5$  throughout the training. The network is trained using a single GPU of NVidia GTX 2080TI.

### 4.3 Experimental Results

In this section we do relevant experiments to verify the effectiveness of our method. We evaluate the AP and AP50 of instance segmentation tasks, and the results are shown in Table 2. We compare our method with MaskRCNN [He *et al.*, 2017] and Lklnet [Girshick *et al.*, 2018]. MaskRCNN is the main method for two-stage instance segmentation, it has high accuracy but slow speed. Our method is a one-stage instance segmentation method, it has lower accuracy than the one-stage method, but it is faster and more suitable for autonomous driving.

| Method      | Backbone         | AP50  | AP    | Time          |
|-------------|------------------|-------|-------|---------------|
| MRCNN       | ResNet101+FPN+FL | 39.14 | 20.26 | 1s            |
| MRCNN       | ResNet50+FPN     | 19.86 | 8.80  | 0.5s          |
| Lklnet      | ResNet101+FPN    | 22.88 | 8.05  | 0.15s         |
| <b>Ours</b> | VGG16+FPN+FL     | 35.42 | 14.28 | <b>0.076s</b> |

Table 2: Instance Segmentation Results. FL is focal loss, MRCNN is MaskRCNN

Specific to different objects, the results of our method are shown in Table 3. The car has the highest accuracy and the rider has the lowest accuracy.

|      | car    | person | cyclist | average |
|------|--------|--------|---------|---------|
| AP50 | 0.4627 | 0.3158 | 0.2842  | 0.3542  |

Table 3: Specific Accuracy

We also evaluated our method on 3D object detection tasks, and the results are shown in Table 4. We compared our method with MonoFENet [Bao *et al.*, 2019] and M3D-RPN [Brazil and Liu, 2019].

|             | Easy  | Moderate | Hard | Time         |
|-------------|-------|----------|------|--------------|
| MonoFENet   | 8.35  | 5.14     | 4.10 | 0.15s        |
| M3D-RPN     | 14.76 | 9.71     | 7.42 | 0.16s        |
| <b>Ours</b> | 9.49  | 5.32     | 4.12 | <b>0.03s</b> |

Table 4: 3D Detection Result. IOU = 0.7, evaluate on car



(a) Origin input image 1248\*384 (b) Pixel-level depth map 312\*96 (c) 3D-Mask fused output 1248\*384

Figure 5: **Results Samples** Results on KITTI datasets. Fig.(a) input of SDOD; Fig.(b) pixel-level depth categories map; Fig.(c) fused instance segmentation and detection output. We use random colors for instance segmentation. In Fig (b) the darker the color of a pixel is, the greater the depth value of a pixel is, and the farther the pixel is from us.

#### 4.4 Ablation Study

In the instance-level and pixel-level depth estimation, we use Equation 1 to discretize the depth into  $K$  categories. We set  $K$  to different values for comparison experiments, and the results are shown in Table 5. The results show that the larger  $K$  is, the more accurate the discrete depth value is, and the higher the accuracy of instance segmentation is. But with the increase of  $K$  time will increase too.

We use object’s length and observation angle to calculate depth threshold, so 3D detection is necessary for instance segmentation. If we set length and observation angle to constant and then we can remove corners regression module and location estimation module. We use the typical values of the target: the length of car is set to 3.5m, person to 0.5m, cyclist to 1m and all objects observation angle is set to be 0. The result is shown in Fig.5.

| Method                 | K   | AP50  | Time   |
|------------------------|-----|-------|--------|
| 3D+Mask                | 64  | 35.42 | 0.076s |
| 3D+Mask                | 128 | 35.95 | 0.089s |
| 2D+Instance depth+Mask | 64  | 33.95 | 0.054s |

Table 5: Ablation Study Results

object detection in real time.

## 5 Conclusion

In this paper, we propose the SDOD framework to combine 3D detection and instance segmentation by depth. In our framework we divide the network into two parallel branches: 3D branch and mask branch, and they are proposal-free. We transform instance segmentation tasks into semantic segmentation tasks by discretizing the object depth into “depth categories”. We combine unreal masks with real depth to train mask branch to solve the problem of imbalanced labels. And our network conducts instance segmentation and 3D

## References

- [Acuna *et al.*, 2018] David Acuna, Huan Ling, Amlan Kar, and Sanja Fidler. Efficient interactive annotation of segmentation datasets with polygon-rnn++. In *CVPR*, 2018.
- [Bao *et al.*, 2019] Wentao Bao, Bin Xu, and Zhenzhong Chen. Monofenet: Monocular 3d object detection with feature enhancement networks. *IEEE Transactions on Image Processing*, 2019.
- [Bolya *et al.*, 2019] Daniel Bolya, Chong Zhou, Fanyi Xiao, and Yong Jae Lee. Yolact++: Better real-time instance segmentation. *arXiv preprint arXiv:1912.06218*, 2019.
- [Brazil and Liu, 2019] Garrick Brazil and Xiaoming Liu. M3d-rpn: Monocular 3d region proposal network for object detection. In *ICCV*, 2019.
- [Chen *et al.*, 2017] Xiaozhi Chen, Huimin Ma, Ji Wan, Bo Li, and Tian Xia. Multi-view 3d object detection network for autonomous driving. In *CVPR*, 2017.
- [Fu *et al.*, 2018] Huan Fu, Mingming Gong, Chaohui Wang, Kayhan Batmanghelich, and Dacheng Tao. Deep ordinal regression network for monocular depth estimation. In *CVPR*, 2018.
- [Geiger *et al.*, 2012] Andreas Geiger, Philip Lenz, and Raquel Urtasun. Are we ready for autonomous driving? the kitti vision benchmark suite. In *ICCV*, 2012.
- [Girshick *et al.*, 2018] Ross Girshick, Ilija Radosavovic, Georgia Gkioxari, Piotr Dollár, and Kaiming He. Detectron. <https://github.com/facebookresearch/detectron>, 2018.
- [He *et al.*, 2017] Kaiming He, Georgia Gkioxari, Piotr Dollár, and Ross Girshick. Mask r-cnn. In *ICCV*, 2017.
- [Huang *et al.*, 2019] Zhaojin Huang, Lichao Huang, Yongchao Gong, Chang Huang, and Xinggang Wang. Mask scoring r-cnn. In *CVPR*, 2019.
- [Kendall *et al.*, 2017] Alex Kendall, Hayk Martirosyan, Saumitro Dasgupta, Peter Henry, Ryan Kennedy, Abraham Bachrach, and Adam Bry. End-to-end learning of geometry and context for deep stereo regression. In *ICCV*, 2017.
- [Kingma and Ba, 2014] Diederik P Kingma and Jimmy Ba. Adam: A method for stochastic optimization. *arXiv preprint arXiv:1412.6980*, 2014.
- [Krizhevsky *et al.*, 2012] Alex Krizhevsky, Ilya Sutskever, and Geoffrey E Hinton. Imagenet classification with deep convolutional neural networks. In *Advances in neural information processing systems*, pages 1097–1105, 2012.
- [Li *et al.*, 2017] Yi Li, Haozhi Qi, Jifeng Dai, Xiangyang Ji, and Yichen Wei. Fully convolutional instance-aware semantic segmentation. In *CVPR*, 2017.
- [Lin *et al.*, 2017a] Tsung-Yi Lin, Piotr Dollár, Ross Girshick, Kaiming He, Bharath Hariharan, and Serge Belongie. Feature pyramid networks for object detection. In *CVPR*, 2017.
- [Lin *et al.*, 2017b] Tsung-Yi Lin, Priya Goyal, Ross Girshick, Kaiming He, and Piotr Dollár. Focal loss for dense object detection. In *ICCV*, 2017.
- [Liu *et al.*, 2016] Wei Liu, Dragomir Anguelov, Dumitru Erhan, Christian Szegedy, Scott Reed, Cheng-Yang Fu, and Alexander C Berg. Ssd: Single shot multibox detector. In *ECCV*, 2016.
- [Long *et al.*, 2015] Jonathan Long, Evan Shelhamer, and Trevor Darrell. Fully convolutional networks for semantic segmentation. In *ICCV*, 2015.
- [Mousavian *et al.*, 2017] Arsalan Mousavian, Dragomir Anguelov, John Flynn, and Jana Kosecka. 3d bounding box estimation using deep learning and geometry. In *CVPR*, 2017.
- [Neven *et al.*, 2019] Davy Neven, Bert De Brabandere, Marc Proesmans, and Luc Van Gool. Instance segmentation by jointly optimizing spatial embeddings and clustering bandwidth. In *CVPR*, 2019.
- [Qin *et al.*, 2019] Zengyi Qin, Jinglu Wang, and Yan Lu. Monogmet: A geometric reasoning network for monocular 3d object localization. In *AAAI*, 2019.
- [Redmon *et al.*, 2016] Joseph Redmon, Santosh Divvala, Ross Girshick, and Ali Farhadi. You only look once: Unified, real-time object detection. In *CVPR*, 2016.
- [Ren *et al.*, 2015] Shaoqing Ren, Kaiming He, Ross Girshick, and Jian Sun. Faster r-cnn: Towards real-time object detection with region proposal networks. In *Advances in neural information processing systems*, pages 91–99, 2015.
- [Sermanet *et al.*, 2013] Pierre Sermanet, David Eigen, Xiang Zhang, Michaël Mathieu, Rob Fergus, and Yann LeCun. Overfeat: Integrated recognition, localization and detection using convolutional networks. *arXiv preprint arXiv:1312.6229*, 2013.
- [Simonyan and Zisserman, 2014] Karen Simonyan and Andrew Zisserman. Very deep convolutional networks for large-scale image recognition. *arXiv preprint arXiv:1409.1556*, 2014.
- [Teichmann *et al.*, 2018] Marvin Teichmann, Michael Weber, Marius Zoellner, Roberto Cipolla, and Raquel Urtasun. Multinet: Real-time joint semantic reasoning for autonomous driving. In *2018 IEEE Intelligent Vehicles Symposium (IV)*, pages 1013–1020. IEEE, 2018.
- [Tian *et al.*, 2019] Zhi Tian, Chunhua Shen, Hao Chen, and Tong He. Fcos: Fully convolutional one-stage object detection. In *ICCV*, 2019.
- [Wang *et al.*, 2019] Xinlong Wang, Tao Kong, Chunhua Shen, Yuning Jiang, and Lei Li. Solo: Segmenting objects by locations. *arXiv preprint arXiv:1912.04488*, 2019.
- [Yu and Koltun, 2015] Fisher Yu and Vladlen Koltun. Multi-scale context aggregation by dilated convolutions. *arXiv preprint arXiv:1511.07122*, 2015.